Electronic Supplementary Information (ESI)

for

Real-time dark-field light scattering imaging to monitor the coupling reaction with gold nanorods as optical probe

Hong Zhi Zhang,[a] Rong Sheng Li,[a] Peng Fei Gao,[a] Ni Wang,[a] Gang Lei,[a] Cheng Zhi Huang[a,b*] and Jian Wang[a*]

a. Education Ministry Key Laboratory on Luminescence and Real-Time Analysis, College of Pharmaceutical Science, Southwest University, Chongqing 400715, China. E-mail: chengzhi@swu.edu.cn; wj123456@swu.edu.cn, Tel:(+86) 23 68254059, Fax:(+86) 23 68866796.

b. Chongqing Key Laboratory of Biomedical Analysis (Southwest University), Chongqing Science & Technology Commission, College of Chemistry and Chemical Engineering, Southwest University, Chongqing 400715,China.

1. Supplementary information for experimental details

1.1 The co-localization technique

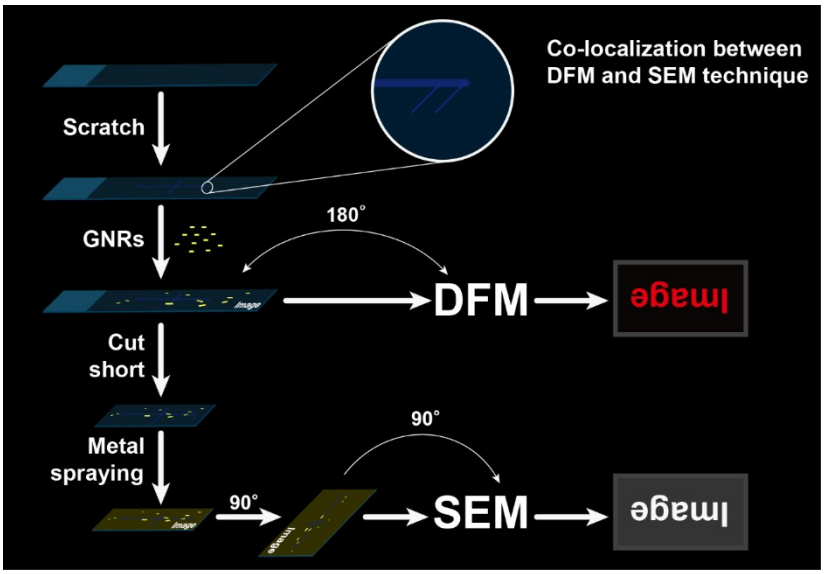

Scheme S1 Schematic illustration of the co-localization of SEM and DFM for GNRs.

The co-localization technique is vividly presented in Scheme S1, which contains the following steps:

1) The glass slides were cleaned with chromic acid and water, and then dried under nitrogen atmosphere.

2) The glass slides were scratched with diamond pen. It is essential that the scratch should include thick cross and the hairline scratch. Wherein, the thick cross should be drawn emphatically in the middle of glass slides, which could be observed by naked eyes. Nevertheless, the hairline scratches were sliced as slight as possible at the end of the cross, which were able to observe under DFM or SEM.

3) It is necessary to remove the glass fragment resulting from scratching, because the size of the glass fragment is similar to that of GNRs, which may interference the imaging effect.

4) GNRs were deposited onto the surface of glass slides.

5) To image, the focus was shifted to the end of hairline scratch to mark the position of GNRs, so that GNRs can be found under microscope readily. Besides, the DFM is inverted, so the images in DFM are the inversion of samples.

6) The glass slides were cut short for SEM.

7) The glass slides were sprayed with gold for 30 s to improve the electric conduction.

8) The glass slides were deasil rotated 90° since the imaging of SEM are clockwise-rotated 90^{o} against the samples, so that the SEM imaging would be inverted as same as the DFM imaging. Herein, 1.5K amplification in SEM was employed to find the same location in DFM.

1.2 The procedure for the etching of the GNRs bulk

Firstly, GNRs were purified by centrifugation at 7,000 rpm for 30 min followed by the removal of the supernatant. Secondly, 0.1 nM GNRs were etched with Fe^{3+} (0.05 mM), HCl (0.03 M) and TU (1 mM). Herein, the etching time was measured in different ways. For example, if etching time was set as 40 min, when GNRs were etched for 30 min, they suffered from centrifugation at 10,000 rpm for 5 min to remove the etching reagents, which was resuspend with water and repeated the centrifugation again. Finally, the DFM, TEM and SEM imaging for GNRs bulk were performed.

2. Supplementary information for theoretical calculation

2.1 The spontaneous reaction of the coupling process

Additionally, we have theoretically calculated the spontaneous degree of the coupling process

As well known from the Fundamental Chemistry:

$$\Delta G_1 = \Delta G_1^{\theta} + RT\ln Q_1 \quad (1)$$

$$\Delta G_2 = \Delta G_2^{\theta} + RT\ln Q_2 \quad (2)$$

$$Q_1 = \frac{\frac{c_{Au^+}}{c^{\theta}} \cdot \frac{c_{Fe^{2+}}}{c^{\theta}}}{\frac{c_{Fe^{3+}}}{c^{\theta}}} \quad (3)$$

$$Q_2 = \frac{\frac{c_{Au[CS(NH_2)_2]_2^+}}{c^{\theta}}}{\frac{c_{Au^+}}{c^{\theta}} \cdot \left[\frac{c_{CS(NH_2)_2}}{c^{\theta}}\right]^2} \quad (4)$$

If the reaction is spontaneous, it needs:

$$\Delta G_1 + \Delta G_2 \le 0 \quad (5)$$

Substitute (1) and (2) into (5)

$$\Delta G_1^{\theta} + \Delta G_2^{\theta} + RT\ln Q_1 Q_2 \le 0 \quad (6)$$

According to (3) and (4),

$$Q_1 \cdot Q_2 = \frac{\frac{c_{Au^+}}{c^{\theta}} \cdot \frac{c_{Fe^{2+}}}{c^{\theta}}}{\frac{c_{Fe^{3+}}}{c^{\theta}}} \cdot \frac{\frac{c_{Au[CS(NH_2)_2]_2^+}}{c^{\theta}}}{\frac{c_{Au^+}}{c^{\theta}} \cdot \left[\frac{c_{CS(NH_2)_2}}{c^{\theta}}\right]^2} = \frac{c_{Au^+} \cdot c_{Fe^{2+}}}{c_{Fe^{3+}}} \cdot \frac{c_{Au[CS(NH_2)_2]_2^+}}{c_{Au^+}[c_{CS(NH_2)_2}]^2} = \frac{c_{Fe^{2+}}}{c_{Fe^{3+}}} \cdot \frac{c_{Au[CS(NH_2)_2]_2^+}}{[c_{CS(NH_2)_2}]^2} \quad (7)$$

According to (6)

$$Q_1 \cdot Q_2 \le e^{-\frac{(\Delta G_1^{\theta} + \Delta G_2^{\theta})}{RT}}$$

That is,

$$\frac{c_{Fe^{2+}}}{c_{Fe^{3+}}} \cdot \frac{c_{Au[CS(NH_2)_2]_2^+}}{[c_{CS(NH_2)_2}]^2} \le e^{-\frac{(\Delta G_1^{\theta} + \Delta G_2^{\theta})}{RT}}$$

When it begins, $c_{Fe^{2+}}$ and $c_{Au[CS(NH_2)_2]_2^+}$ is near to zero and $c_{Fe^{3+}}$ is much more than $c_{Fe^{2+}}$. $c_{Fe^{3+}} = 0.05\text{mM}$; $c_{CS(NH)_2} = 1\text{mM}$.

Then,

$$\frac{c_{Fe^{2+}}}{c_{Fe^{3+}}} \cdot \frac{c_{Au[CS(NH_2)_2]_2^+}}{[c_{CS(NH_2)_2}]^2} \approx 0 \text{, and } \Delta G_1^\theta + \Delta G_2^\theta < 0$$

Thus, the coupling reaction is spontaneous to perform.

When it reaches equilibrium, it exists:

$$\Delta G_1 + \Delta G_2 = 0$$

$$\Delta G_1^\theta + \Delta G_2^\theta + RT\ln Q_1 Q_2 = 0$$

$$\frac{c_{Fe^{2+}}}{c_{Fe^{3+}}} \cdot \frac{c_{Au[CS(NH_2)_2]_2^+}}{[c_{CS(NH_2)_2}]^2} = e^{-\frac{(\Delta G_1^\theta + \Delta G_2^\theta)}{RT}} = 2.83\times10^3$$

$$\frac{c_{Fe^{2+}}}{(5\times10^{-5} - c_{Fe^{2+}})} \cdot \frac{c_{Au[CS(NH_2)_2]_2^+}}{[1\times10^{-3} - 2c_{Au[CS(NH_2)_2]_2^+}]^2} = 2.83\times10^3$$

According to the law of conservation of mass and electron conservation,

$$c_{Fe^{2+}} = c_{Au^+} = c_{Au[CS(NH_2)_2]_2^+}$$

That is, $c_{Fe^{2+}}$ =0.0000499 M

The original concentration of Fe^{3+} is 5×10^{-5} M, thus 99.8% Fe^{3+} is converted to Fe^{2+}. That is, the coupling reaction could spontaneously finish as high as 99.8%.

2.2 The Gibbs free energy of KI/I_2 induced chemical etching of GNRs

$$I_2 + 2e^- = 2I^- \quad E^\theta = 0.535\text{V}$$

$$[AuI_2]^- + e^- = Au + 2I^- \quad E^\theta = 0.578\text{V}$$

$$\Delta G = -nFE^\Theta$$

$$\Delta G_{Totol} = -214\text{kJ/mol}$$

Thus, the chemical reaction is thermodynamically spontaneous since the relative Gibbs free energy is negative, which is similar to the result obtained with TU.

3. Supplementary information for investigation results

3.1 Characterization of GNRs.

In order to attain more details of GNRs, absorbance and scattering spectra, as well as the theoretical scattering intensities have been obtained with UV-3600 spectrophotometer, light scattering dark-field spectrometer CCD and FDTD solutions, respectively. The transverse and longitudinal surface plasmon absorption bands were at 524 nm and 708 nm (Fig. S1a, ESI†). Furthermore, the experimental and theoretical LSPR scattering spectrum peak of GNRs located at 719 nm 712 nm (Fig. S1 b-c, ESI†), which match with each other very well.

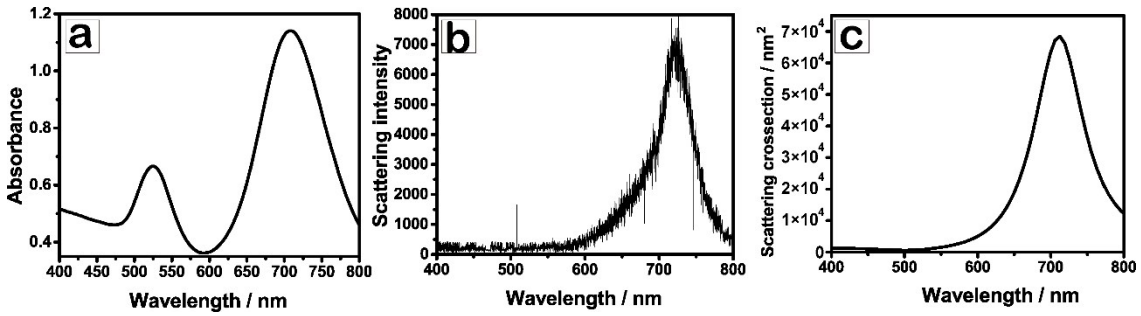

Fig. S1 The characterization of GNRs. a. absorbance spectrum; b. scattering spectrum; c, theoretical scattering spectrum.

3. 2 The mechanism for etching GNRs caused by the coupling reaction

The control work shows that GNRs were hardly etched if in the absence of Fe^{3+} or TU, suggesting that the etching process of GNRs was facilitated with a coupling reaction (Fig. S2, ESI†).

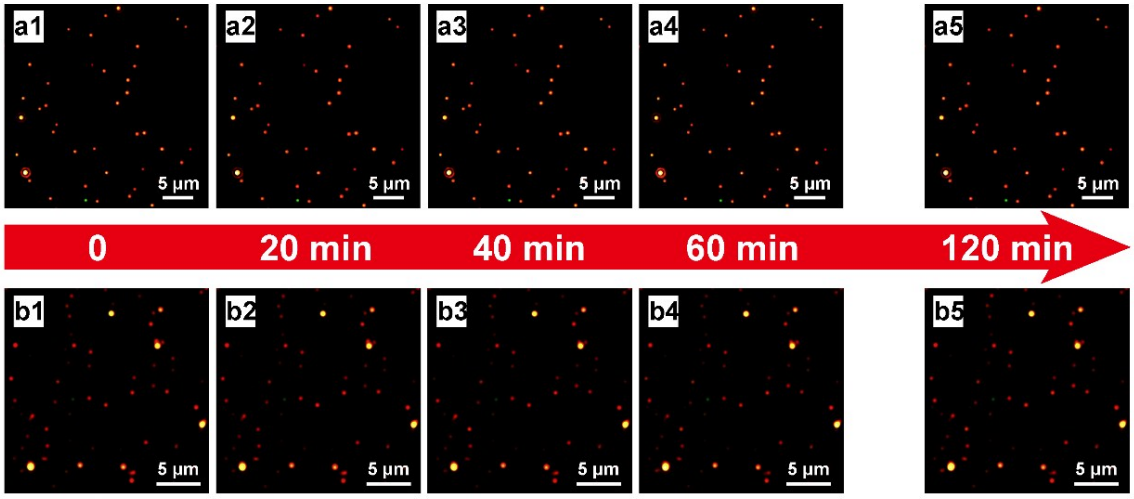

Fig. S2 The control work about GNRs etching process under DFM during long time. Conditions: (a1-a5), AuNRs, 0.01 nM; Fe^{3+}, 0.05 mM; HCl, 0.03 M; (b1-b5), AuNRs, 0.01 nM; TU, 1 mM; HCl, 0.03 M.

The elements change during the coupling reaction was confirmed by X-ray photoelectron spectroscopy (XPS) and FTIR spectra (Fig. S3, ESI†). XPS was performed after mixing GNRs with Fe^{3+} and TU for 60 min. As shown in Fig. S2, the peaks locate at 88.4 eV and 84.5 eV could be assigned to Au_{4f}, [1, 2] which suggested that the original Au^0 of GNRs was partially oxided into Au^+. Besides, the peaks locate at 711.5 eV and 709.7 eV could be attributed to Fe_{2p},[3] indicating that Fe^{3+} was reduced to Fe^{2+}. It is followed that Au^0 of GNRs was oxidized to Au^+ by Fe^{3+}. What's more, in the FTIR spectra, the stretching vibration of C=S group (1400.59 cm^{-1}) shifted to lower wave numbers (1393.29 cm^{-1}) with decreased intensity, suggesting the decrease of C=S groups due to the formation of Au-TU complexes.[4]

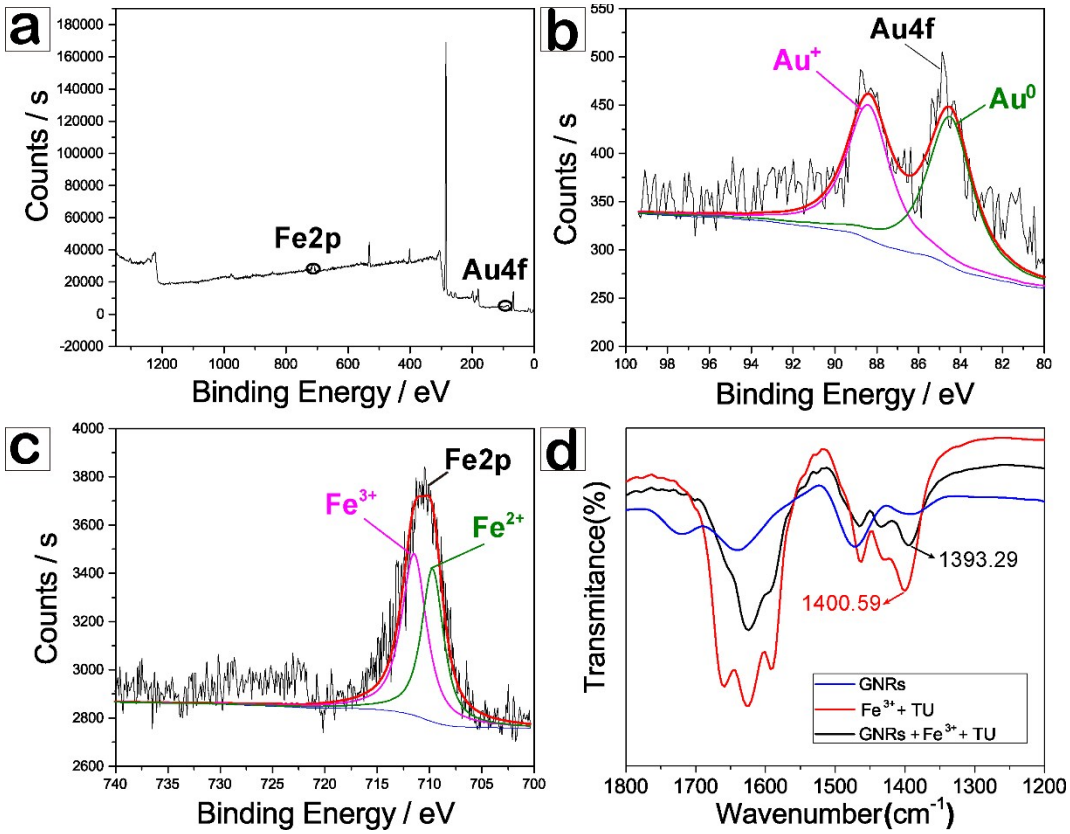

Fig. S3 Characterization of GNRs that reacted with Fe^{3+} and TU. a, The full XPS spectrum; b, Au_{4f} XPS spectrum; c, Fe_{2p} XPS spectrum; d, FTIR spectra.

Then, we investigated the correlations between reaction rate and different concentrations of Fe^{3+} and TU (Fig. S4, ESI†). It is found that the etching process is concentration-dependent. When etching agents at appropriate concentrations were added to etch GNRs, it would take about 60 min to GNRs to transfer the light scattering from red to green. If Fe^{3+} or TU at a lower concentration, the etching process would be prolonged. Comparatively speaking, Fe^{3+} played a dominant role in the etching process due to the oxidation of Fe^{3+} and the complex of Cl^- ligand to promote the formation of $[AuCl_2]^-$, reducing the electron potential of gold species, which enabled Fe^{3+} to further shorten GNRs.[5] But TU played a secondary function in the etching of GNRs, which did not dramatically shorten the time to etch GNRs if its concentration was higher than 1 mM.

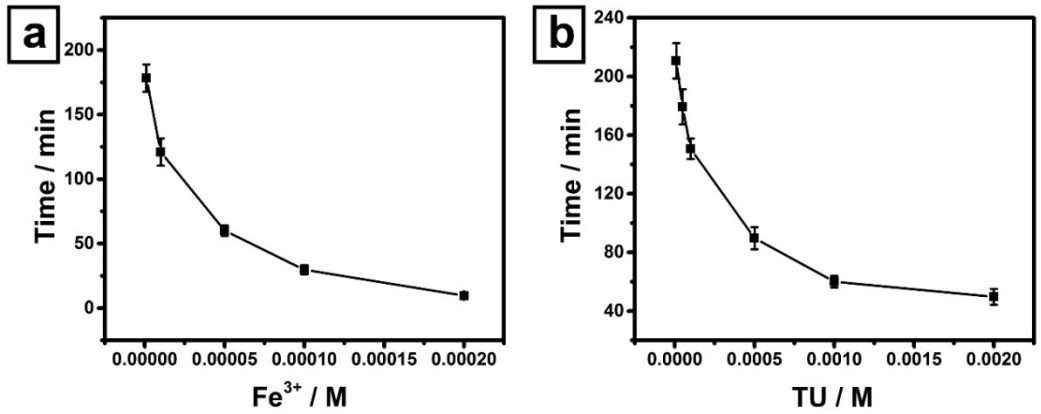

Fig. S4 The correlations between reaction rate and etching agents. a, the etching process adjusted by Fe^{3+}. Conditions: Fe^{3+}: 1 μM, 10 μM, 50 μM, 100 μM and 200 μM; AuNRs, 0.01 nM; HCl, 0.03 M; TU, 1 mM. b, the etching process adjusted by TU. Conditions: TU: 10 μM, 50 μM, 100 μM, 500 μM, 1 mM and 2 mM. AuNRs, 0.01 nM; Fe^{3+}, 0.05 mM; HCl, 0.03 M.

Besides the etching reagents, the acidity of solution could affect the etching process (Fig. S5, ESI†). When HCl was adjusted to 0.003 M, the etching process could go on, which was similar to the previous result (0.03 M HCl). While the concentration of HCl was lowered to 0.0003 M, the etching process would stop gradually. If HCl was as low as 0.00003 M, the etching process would stop immediately, which was attributed to the formation of $Fe(OH)_3$ to reduce the oxidizing ability of Fe^{3+}.

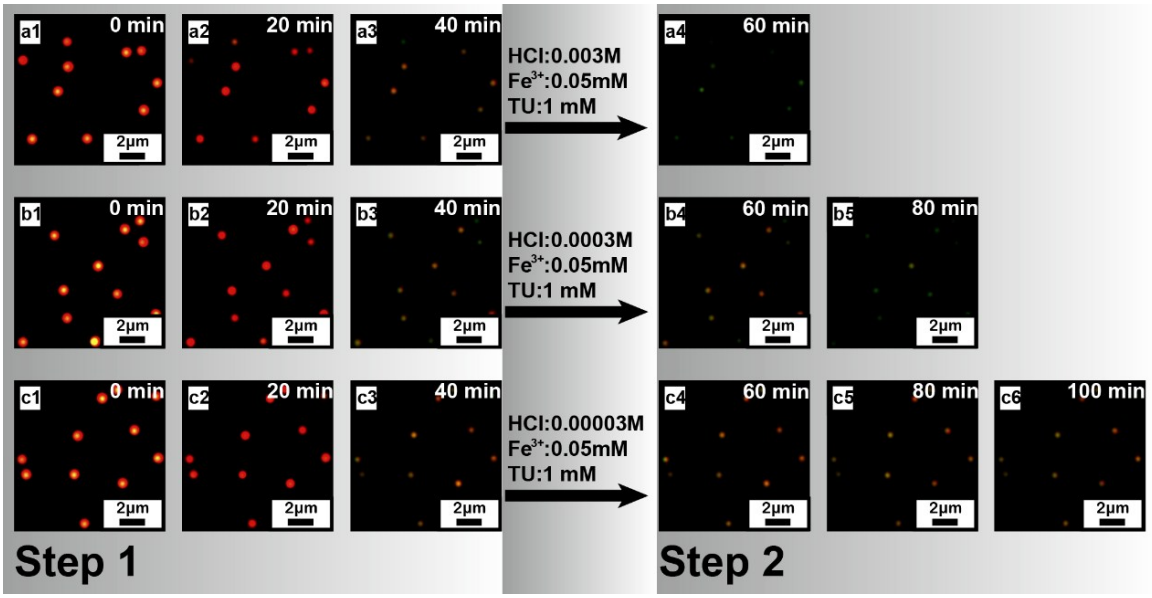

Fig. S5 DFM evolution of GNRs during the coupling reaction process. Conditions: (a1-a3; b1-b3; c1-c3), AuNRs, 0.01 nM; Fe^{3+}, 0.05 mM; HCl, 0.03 M; TU, 1 mM; (a4; b4-b5; c4-c6), AuNRs, 0.01 nM; Fe^{3+}, 0.05 mM; TU, 1 mM; HCl, (a4),0.003 M, (b4-b5),0.0003 M, (c4-c6),0.00003 M.

To attain more details about the DFM in the progress of the coupling reaction, the GRB of each GNR in Fig. 3 a2-d2 was analyzed in the manner of wind rose. The percents of digital RGB values (V) are calculated using the following equations:

$$P_R = V_R/(V_R + V_G + V_B)$$

$$P_G = V_G/(V_R + V_G + V_B)$$

$$P_B = V_B/(V_R + V_G + V_B) = 1 - P_R - P_G$$

Wherein, P_R, P_G and P_B represent the percentages of red (R), green (G) and blue (B) color values (V_R, V_G, and V_B) of a given GNRs, respectively. The result showed that the red percentage of GNRs gradually reduced from more than 80% to less than 20% and the green percentage of GNRs gradually increased from less than 20% to more than 70% (Fig. S6, ESI†), which was time-dependent.

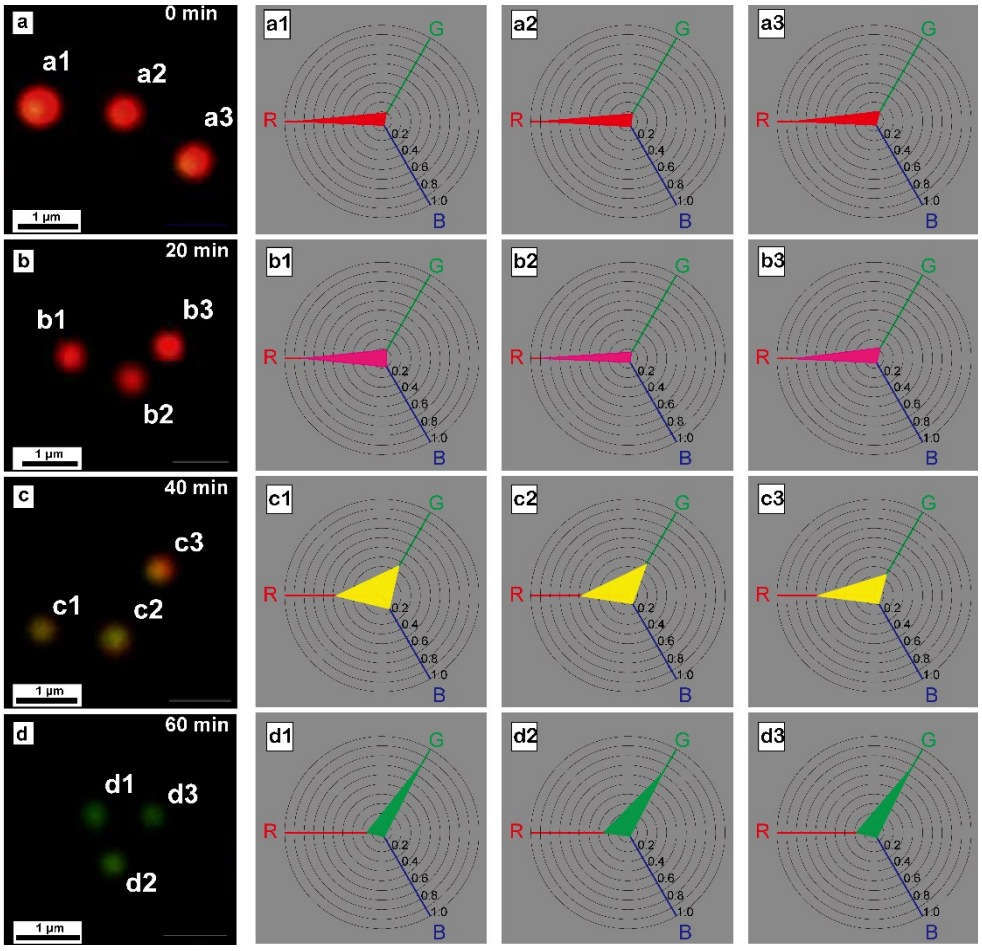

Fig. S6 The RGB wind rose of GNRs in the coupling reaction process. a, 0 min; b, 20 min; c, 40 min; d, 60 min.

The DFM images of GNRs were recorded during the coupling reaction process. The original GNRs presented the strong red light scattering, which turned to weak yellow-green when the coupling reaction carried out for 40 min. Then, Fe^{3+} and TU were washed away, leading to the termination of the coupling reaction (Fig. S7, ESI†). In this case, the chemical etching of GNRs could not occur, making GNRs keep the yellow-green light scattering in the following time.

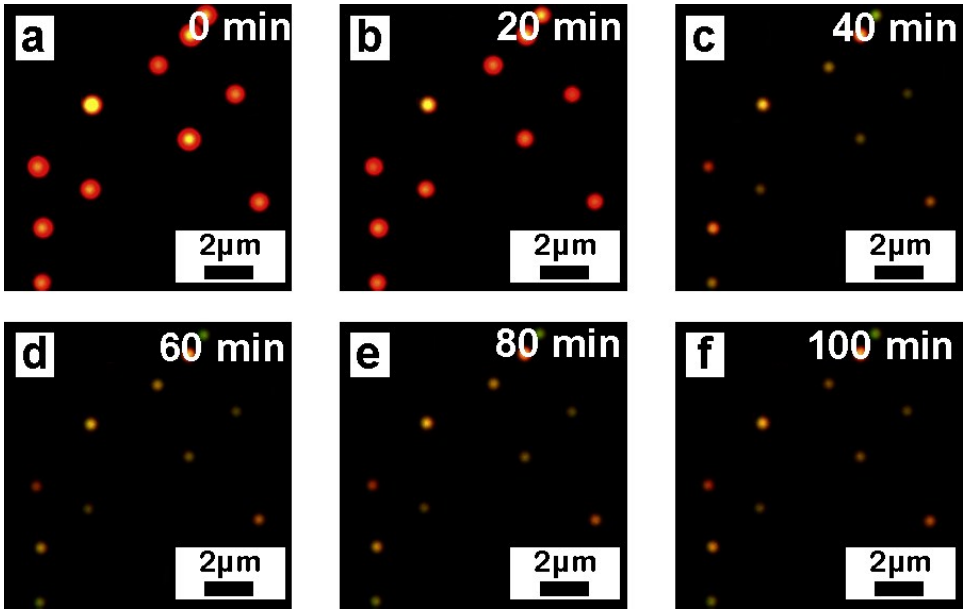

Fig. S7 DFM evolution of GNRs during the coupling reaction process. Conditions: (a-c), AuNRs, 0.01 nM; Fe^{3+}, 0.05 mM; HCl, 0.03 M; TU, 1 mM; (d-f), AuNRs, 0.01 nM, Fe^{3+}, 0 mM; HCl, 0 M; TU, 0 mM.

The 3D-scattered diagram shows the dynamic performance of GNRs in Fig. 3 (a5-d5). In the process of coupling reaction, the red percentage of GNRs in DFM decreased and the green percentage increased greatly, but the blue percentage fluctuated within the range from 0 to 15% (Fig. S8, ESI†).

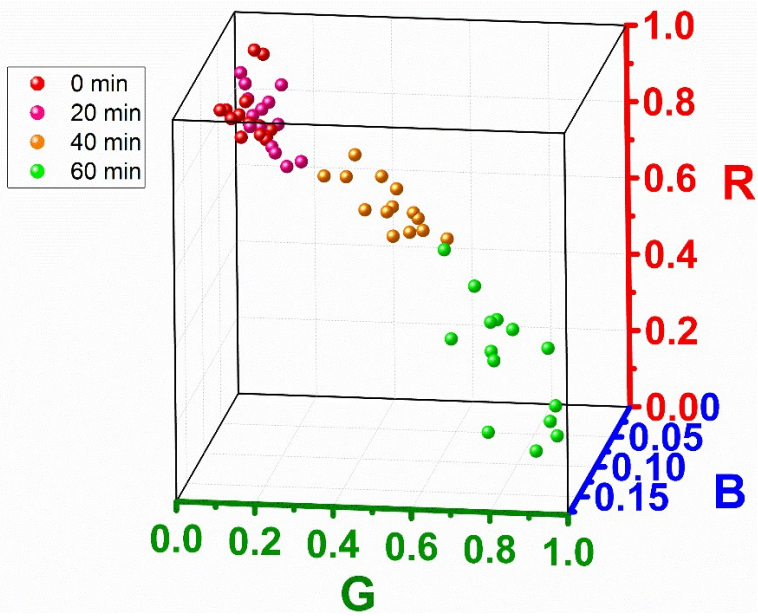

Fig. S8 3D-scattered diagram of the particles from Fig. 4 a5-d5.

3.3 Monitor the coupling process with other sizes of GNRs

In order to find out whether all GNRs could be employed as optical probes to monitor the coupling reaction process, different sizes of GNRs, including the LPRA at 600 nm (purchased from Nanoseedz company), 650 nm and 850 nm (prepared according to the previous report[6]) , were investigated.

Firstly, GNRs with the LPRA at 600 nm were investigated. Under the dark-filed microscopy, GNRs presented the red light scattering, which became yellow and weak green after the coupling reaction carried out for 20 min and 40 min, respectively. Under the SEM, the size of the rod-like GNRs was about 52.6 nm × 85.1 nm, which became shuttle-like with the middle length of 74.5 nm, the side length of 44.8 nm, and the middle diameter of 45.3 nm, if the coupling reaction carried out for 20 min. After another 20 min, they became sphere-like with diameter of 44.6 nm.

Under the same conditions as described in the main text, the hot-spots of the as-prepared GNRs that simulated by FDTD solutions were in the boundary between the side and bottom firstly. Then, the hot-spots of shuttle-like GNRs transferred to the sharp corners (Fig. S9, ESI†). These results are similar to those GNRs with LRPA at 708 nm as probes.

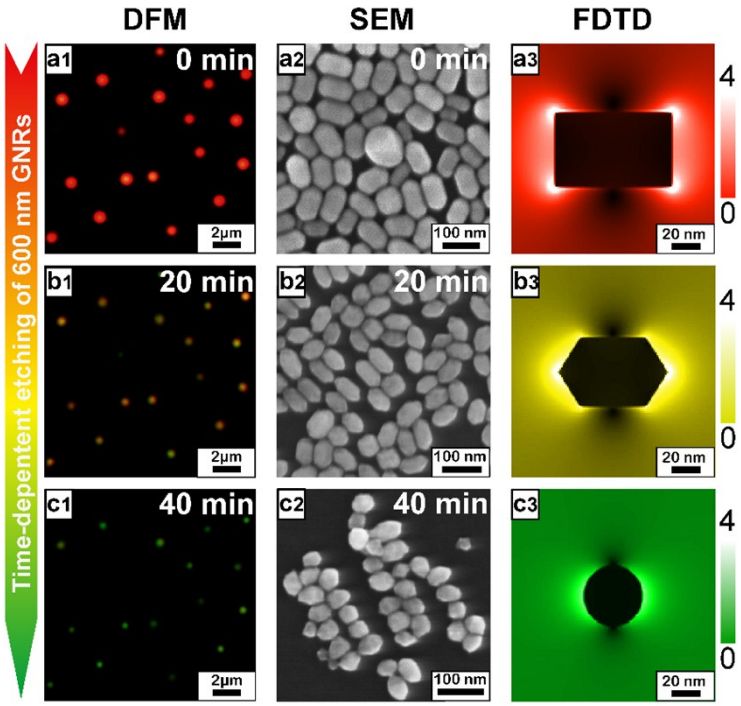

Fig. S9 The process of etching GNRs (LPRA at 600 nm) caused by the coupling reaction. DFM was recorded at 0 min (a1), 20 min (b1) and 40 min (c1). SEM was recorded at 0 min (a2), 20 min (b2) and 40 min (c2). Electromagnetic field amplitude patterns of GNRs was simulated by FDTD. The squared moduli distributions of the electric field intensity of (a3) 0 min, (b3) 20 min and (c3) 40 min as a function of time ($|E(t)|^2$) were calculated under the illumination of a 300-800 nm TFSF light source.

Secondly, GNRs with the LPRA at 650 nm were employed to monitor the coupling process. Under the DFM, the as-prepared GNRs presented red light scattering. And then they became yellow or red-yellow after 20-min reacting with TU and Fe^{3+}. Finally, they displayed green light scattering. Under SEM, the axial length of rod-like GNRs was about 63.2 nm×107.5 nm. After mixing with TU and Fe^{3+} for 20 min, they became shuttle with the middle length of 99.7 nm, the side length of 51.4 nm, and the middle diameter of 60.1 nm. In addition, 40 min later, they became sphere with the diameter of 52.2 nm.

Under the same conditions as the description in the main text, the hot-spots that simulated by FDTD solutions were in the boundary between the side and bottom. Then, the hot-spots of shuttle-like GNRs transferred to the sharp corners and then to sphere. Similar to the GNRs with LPRA at 600 nm, this process showed that the morphological, imaging and FDTD changes of GNRs caused by coupling reaction always followed the same principles, regardless of the sizes of GNRs (Fig. S10, ESI†).

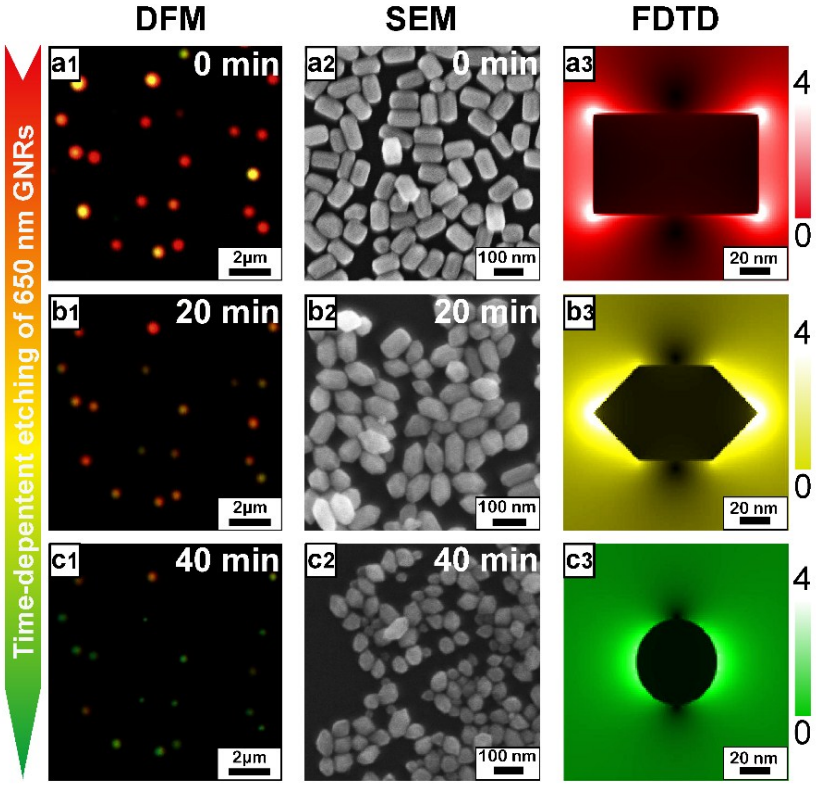

Fig. S10 The process of etching GNRs (LPRA at 650 nm) caused by the coupling reaction. DFM was recorded at 0 min (a1), 20 min (b1) and 40 min (c1). SEM was recorded at 0 min (a2), 20 min (b2) and 40 min (c2). Electromagnetic field amplitude patterns of GNRs was simulated by FDTD solution. The squared moduli distributions of the electric field intensity of (a3) 0 min, (b3) 20 min and (c3) 40 min as a function of time ($|E(t)|^2$) were calculated under the illumination of a 300-800 nm TFSF light source.

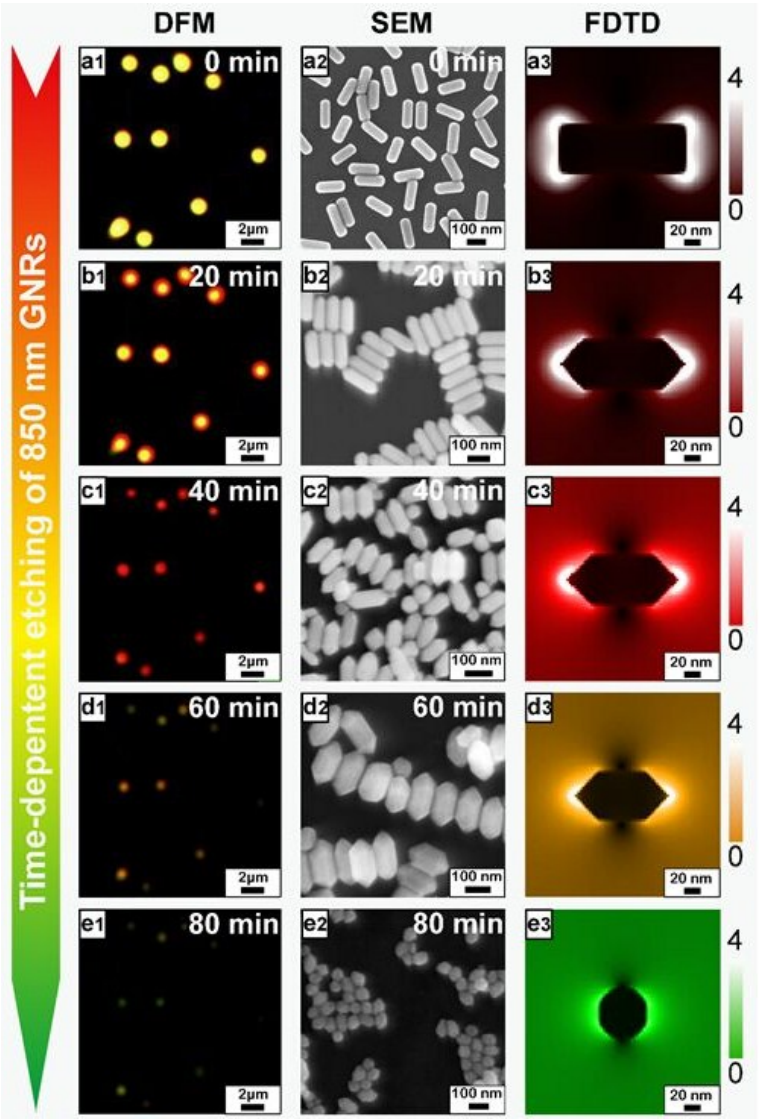

Fig. S11 The process of etching GNRs (LPRA at 850 nm) caused by the coupling reaction. DFM was recorded at 0 min (a1), 20 min (b1), 40 min (c1),60 min (d1) and 80 min (e1). SEM was recorded at 0 min (a2), 20 min (b2), 40 min (c2), 60 min (d2) and 80 min (e2). Electromagnetic field amplitude patterns of GNRs was simulated by FDTD solution. The squared moduli distributions of the electric field intensity of (a3) 0 min, (b3) 20 min , (c3) 40 min, 60 min (d2) and 80 min (e2) as a function of time ($|E(t)|^2$) were calculated under the illumination of a 300-800 nm TFSF light source.

Thirdly, the GNRs with aspect ratios of 4 and the LPRA at 850 nm were employed to indicated the coupling process. Under the DFM, the as-prepared GNRs presented yellow light scattering. Then, it became bright red, dark red, green-yellow and green when the coupling reaction carried out for 20 min, 40 min, 60 min and 80 min, respectively.

Under SEM, the cylindrical GNRs were measured with an axial length of 58.6 nm × 159.1 nm. During the coupling reaction, the shuttle-like nanoparticles appeared, and they then turned to spherical nanoparticles. When the coupling reaction proceeded for

20 min, the size of long shuttle-like GNRs became the middle length of 148.4 nm, the middle diameter of 57.5 nm and the side length of 95.4 nm. 40 min later, GNRs became shuttle-like with the middle length of 134.3 nm, the middle diameter of 57.3 nm and the side length of 74.4 nm. 60 min later, GNRs became short shuttle-like with the middle length of 110.7 nm, the middle diameter of 57.6 nm and the side length of 57.2 nm. Finally, they became spherical nanoparticles with diameter of 28.4 nm.

The FDTD simulation was similar to the FDTD results of other GNRs, which located at the boundary between the side and bottom, and then transferred to the sharp corners of shuttle-like GNRs, and finally to spheral nanoparticles.

Furthermore, the morphologies of GNRs always kept shuttle-like until the hot-spots became weaker and weaker gradually (Fig. S11, ESI†).

3.4 SEM, TEM and DFM images for monitoring the etching GNRs bulk

GNRs were still etched to form shuttle-like morphology when GNRs were deposited with many dense layers (Fig. S12, ESI†).

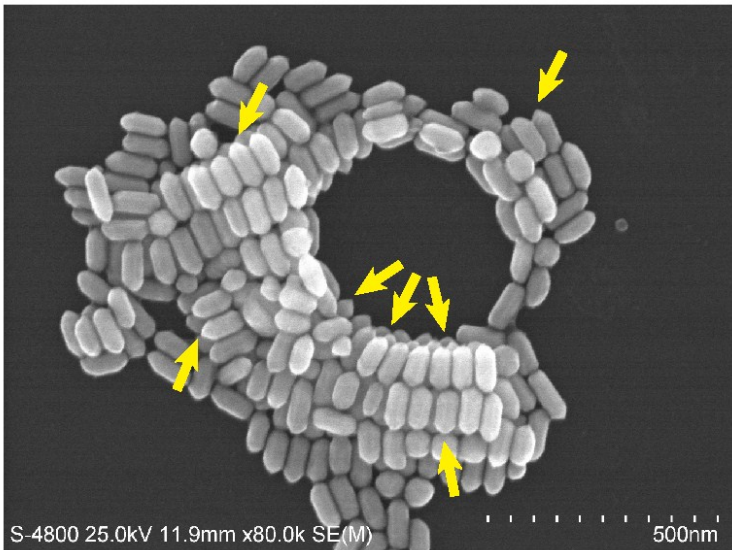

Fig. S12 Monitoring the etching process with many GNRs layers. Conditions: Fe^{3+}, 0.05 mM; TU, 1 mM; HCl, 0.03 M.

As shown in Fig. S13, DFM images present that the light scattering tuned from red to yellow and finally to green, and TEM and SEM images indicate that the morphology of GNRs changed from rod to fusiform and finally to sphere, which are similar to the result obtained from single GNRs on the surface of glass slide.

The difference lies on the etching rate originated from the slight variation of GNRs concentration. Wherein, the unbound GNRs on glass slide surface were washed away to result in a lower concentration of GNRs, which were reacted with the original concentration of etching reagents (0.05 mM Fe^{3+}, 0.03 M HCl and 1 mM TU), leading to a faster etching rate to finish the etching process within 60min. Comparatively speaking, it took 80 min for GNRs bulk to finish the etching process.

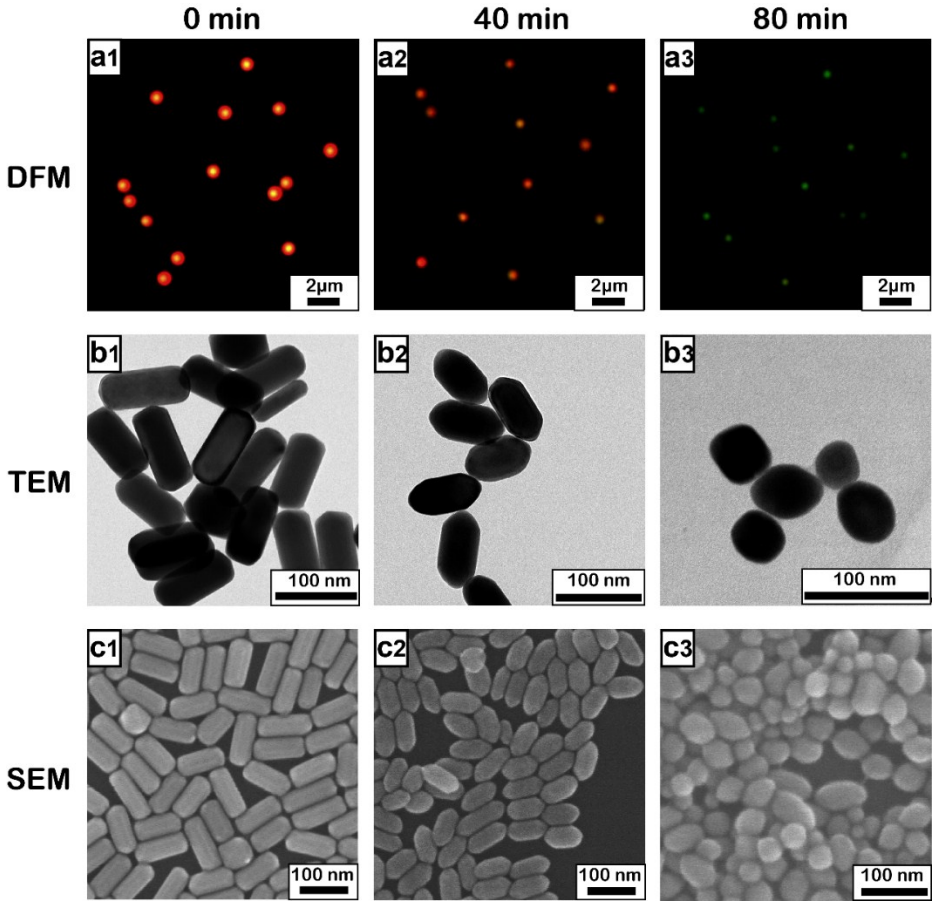

Fig. S13 The coupling reaction induced etching process of GNRs in bulk. a1-a3, DFM images of GNRs; b1-b3, TEM images of GNRs; c1-c3, DFM images of GNRs. Conditions: Fe^{3+}, 0.05 mM; TU, 1 mM; HCl, 0.03 M.

3.5 More details for etching GNRs.

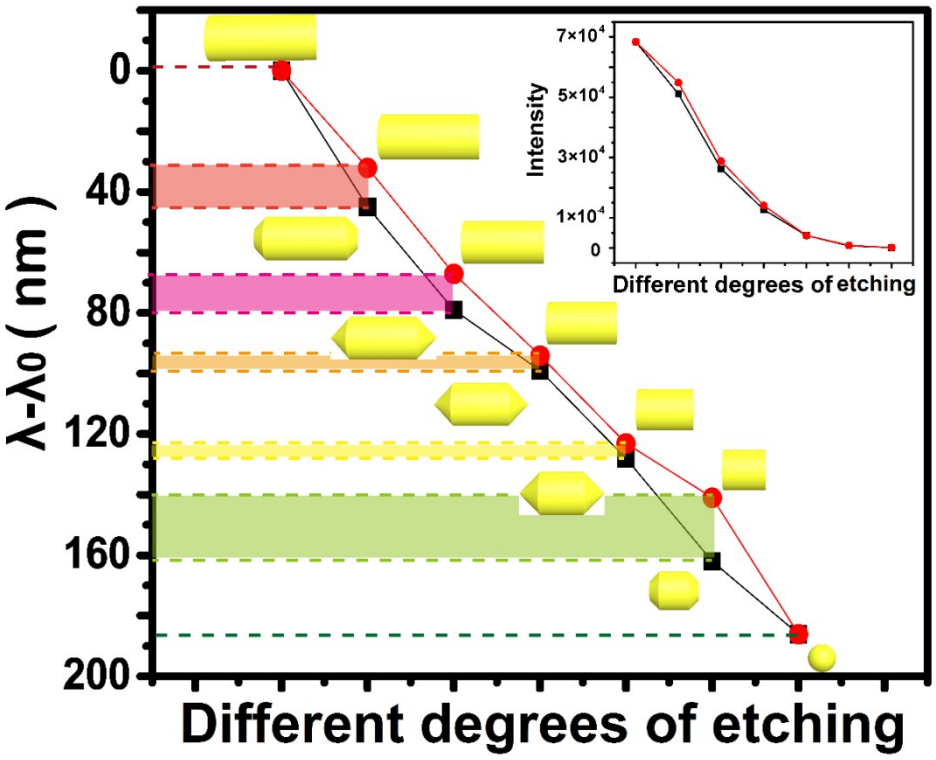

Fig. S14 The spectrum peak shift of the etching process of GNRs induced by different reactions. The inset is the scattering intensity (these data were analyzed from Fig. 6).

In this work, the KI/I_2 system supplies a much greater etching rate than TU (Fig.6), thus we supposed that the rapid etching resulting in the peeling Au layers to yield shorter GNRs without facet selectivity.

More investigation the slow etching of GNRs induced by the coupling reaction is facet selective. The XRD pattern of GNRs presents the intense peaks corresponding to (111), (200) and (220) Bragg reflection, confirming the confirmation of GNRs with the face-centered cubic (fcc) crystal structure. the etching process begins, the percentage of the gold atoms with the Au (111) facet dramatically decreases, possibly suggesting that the etching mainly occurs from Au (111) facet due to the less covered by CTAB, which is probably the most accessible part of GNRs for the chemical etching (Fig. S15).

The TEM imaging and the selected area electron diffraction pattern also prove the facet during the etching process (Fig. S16).

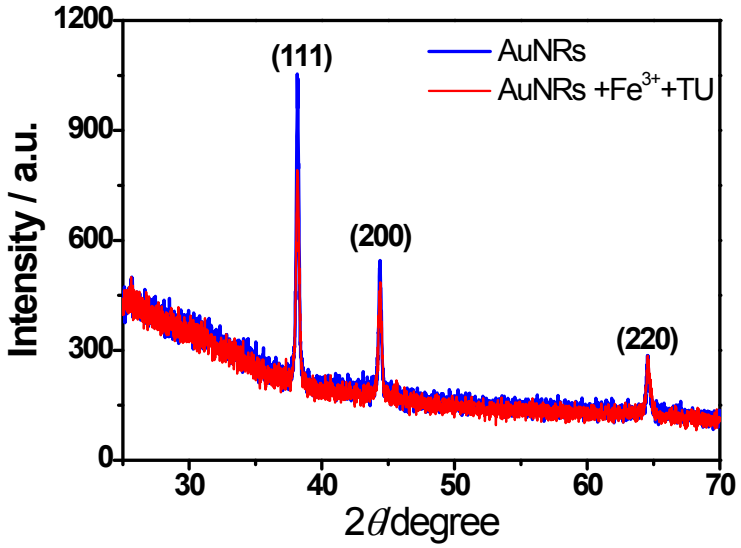

Fig. S15 XRD pattern of GNRs before and after etching.

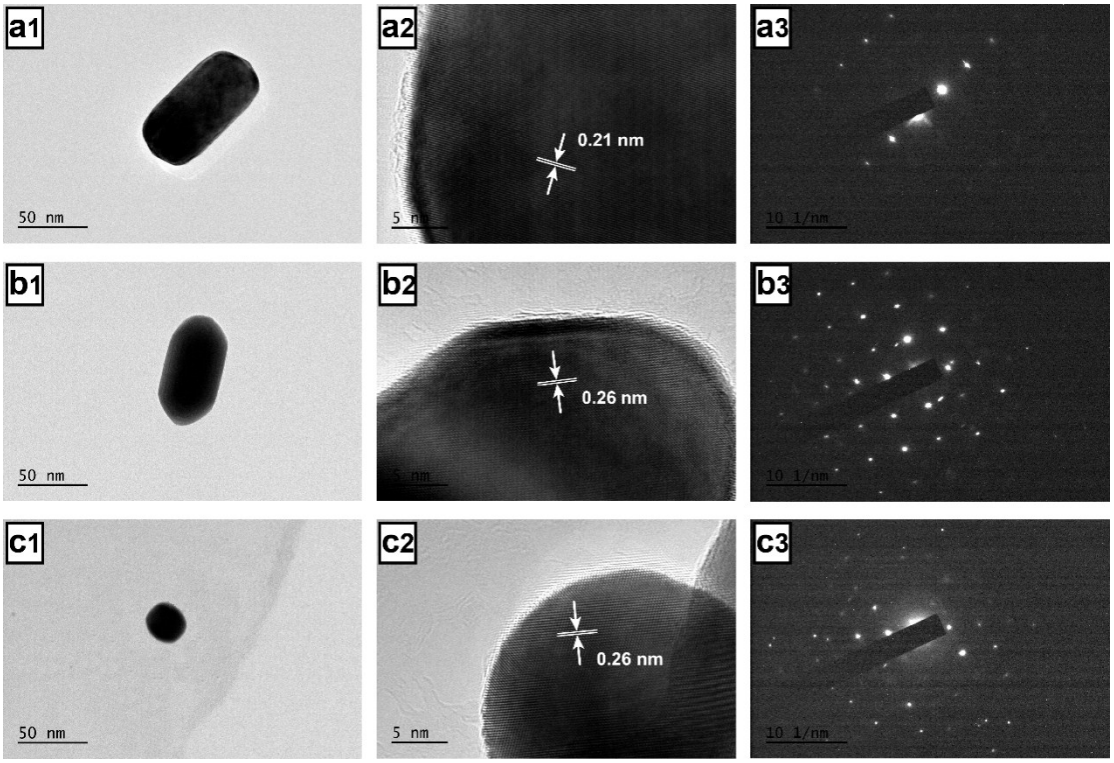

Fig.S16 TEM (a1-c1) and HRTEM (a2-c2) images as well as selected area electron diffraction pattern (a3-c3) of the as-prepared GNRs (a1-a3), the etching resultant nanoparticles with the shape of shuttle (b1-b3) and sphere (c1-c3).

References

1 H. Konno and Y. Yamamoto, *Bull. Chem. Soc. Jpn.*, 1987, 60, 2561-2564.
2 N. H. Turner and A. M. Single, *Surf. Interface Anal.*, 1990, 15, 215-222.
3 J. C. Carver, G. K. Schweitzer and T. A. Carlson, *J. Chem. Phys.*, 1972, 57, 973-982.
4 A. E. Bolzán, T. Iwasita and A. J. Arvia, *J. Electroanal. Chem.*, 2003, 554–555, 49-60.
5 R. X. Zou, X. Guo, J. Yang, D. D. Li, F. Peng, L. Zhang, H. J. Wang and H. Yu, *Crystengcomm*, 2009, 11, 2797-2803.
6 X. C. Ye, C. Zheng, J. Chen, Y. Z. Gao and C. B. Murray, *Nano Lett.*, 2013, 13, 765-771.